International Journal of Nanomaterials, Nanotechnology and Nanomedicine

Wenyuan Liu[1], Changfeng Ke[1], Xuehai Yan[2], Li Duan[1]*, Lin Li[1] and Chong Liu[1]

[1]Northwest Institute of Nuclear Technology, Xi'an, Shaanxi 710024, China
[2]Institute of Process Engineering, CAS, Beijing 100190, China

Dates: **Received:** 13 April, 2015; **Accepted:** 09 May, 2015; **Published:** 11 May, 2015

***Corresponding author:** Li Duan, Institute of Process Engineering, CAS, Beijing 100190, China, E-mail: duanli@iccas.ac.cn

www.peertechz.com

ISSN: 2455-3492

Keywords: Thin film batteries; Lithium-ion batteries; Nanocomposite materials; Anode; Electrochemical properties

Research Article

LiF-MO (M=Co, Fe, Ni) Nanocomposite Thin Film as Anode Materials for Lithium-ion Battery

Abstract

To investigate the electrochemical performance of MO (M=Co, Fe, Ni) nanostructures on lithium insertion and extraction, size-controlled LiF-MO nanocomposite thin-film electrodes, consisting of metallic M and M oxide (MO) nanoparticles in an amorphous, inert LiF matrix, were designed and fabricated using a RF sputtering system with metallic M and LiF mixture targets. The structural and electrochemical properties of nanocomposite thin-film electrodes were characterized using TEM, SAED, XRD, XPS, and electrochemical measurements. The results showed that MO particles with average particle sizes of ca.10nm were well-dispersed in LiF matrix to form a kind of homogeneous LiF-MO nanocomposite by the sputtering method. The inert medium of LiF provides an effective matrix to prevent the crystallization and agglomeration of MO during the deposition and electrochemical cycling of the thin film electrode, and then the well-formed nanophase structure in the nanocomposite thin-film electrodes leads to an excellent electrochemical cycling performance with the stable discharge specific capacity above 300mAh/g.

Introduction

There has been intense interest in developing new anode materials that store higher densities of lithium for secondary lithium batteries. Rock salt structured MO-type (M = Cu, Fe, Co, Ni) transition metal oxides have been considered as a promising anode because of its high capacity (~700 mAh/g), and excellent recyclibility (up to 100 cycles) toward lithium [1-6]. Recently, the introduction of nano-sized materials in battery systems has been suggested to be a possibility since the physical, electrical and chemical properties of nano-phases are very different from those of their bulk counterparts [7-9]. It is believed that the key to the successful application of nanostructured electrodes in batteries is a combination of a number of reaction sites, a short transport pathway for electrons and ions, and improving cycle performance of the battery. However, most studies reported previously have focused on bulk materials and few have dealt with the performance of these oxides in thin film electrodes. Thin-film electrodes are ideal models for understanding the relationship between electrode properties and electrochemical behavior because they do not usually contain a binder [10-12]. Moreover, thin-film electrodes can be applied directly into thin-film batteries. So far, we have designed and fabricated some kinds of thin-film lithium batteries with excellent electrochemical properties [13-15]. Currently, MO thin films are typically prepared by reactive sputtering or pulse laser deposition (PLD) using a single metal target [10,11]. The lack of uniformity over a large area is the major drawback for PLD [11]. Therefore, sputtering may be a suitable alternative process for making MO thin films. However, it is difficult to directly fabricated the nanostructured MO thin films with a particles size of less than several tens of nanometers by sputtering due to a plasma heating effect. Furthermore, it may be more important to keep the nanostructured stability to improve the electrode cycling performance during lithium insertion and extraction [1-3]. There are some evidences that nanocomposite thin-film electrodes consisting of electrochemical active nano-sized particles embedded into an inactive "buffer matrix" undergo better capacity retention than single thin film during cycling [16,17].

It is well-known that LiF possesses chemical and electrochemical inertia, and may be used as a buffer matrix to compensate for the expansion and shrinkage of metal oxide during electrochemical cycling, thus preventing the aggregation of nanostructured metal oxide during charging/discharging. In this work, we have investigated the preparation and electrochemical properties of LiF-MO, a two-phase nanocomposite thin films electrode, i.e., MO nanodots embedded in a LiF matrix prepared by a sputtering system. It is shown that the addition of inert LiF matrix effectively reduce the particles size of MO and improves the cycling performance of lithium-ion batteries.

Experimental

Preparation of the nanocomposite thin films

LiF-MO nanocomposite thin films were prepared on the stainless steel substrates by reactive RF magnetron sputtering. A sputtering chamber was evacuated below 5×10-4 Pa with a turbo-molecular pump and a mechanical pump. Composite targets consisting LiF and M (M= Fe, Co, and Ni) were obtained as targets by cold pressing LiF power (99% Aldrich) and a high pure metal(99.99%) power with the molar ratio of 1:1. Before film deposition, the target was pre-sputtered for 30 minutes to remove the target surface contaminations. The gas mixtures, high purity O2 and Ar with the ratio of 1 to 5, were introduced into sputtering chamber by a mass flow controller. The gas flow was regulated to maintain the chamber pressure at approximately 1.0 Pa. The target-substrate distance was maintained at 60 mm. Sputtering was performed at the RF power of 25 W at room temperature.

Assembly of the Li-ion cells

For the electrochemical measurements, the cells were constructed by using the as-deposited nanocomposites LiF-MO thin films as a working electrode and two lithium sheets as a counter electrode and a reference electrode, respectively. The electrolyte consisted of 1 M LiPF6 in a nonaqueous solution of ethylene carbonate (EC) and dimethyl carbonate (DMC) with a volume ratio of 1:1 (Merck). The cells were assembled in an Ar filled glove box. Charge-discharge measurements were performed at room temperature with a Land BT 1-40 battery test system. The cells were cycled between 0.01 and 3.5 V vs. Li/Li+ at a current density of 28 μA/cm^2.

Characterisation

X-ray diffraction (XRD) patterns of the thin film electrodes were recorded by a Rigata/max-C diffractometer with Cu-Kα radiation. The weights of thin films were examined by electrobalance (BP 211D, Sartorius). X-ray photo-electron spectroscopy (XPS) measurements were performed on a Parkin Elmer PHI 6000C ECSA system with monochromatic Al Kα (1486.6 eV) irradiation. To correct possible charging of the films by X-ray irradiation, the binding energy was calibrated using the C1s (284.6 eV) spectrum of hydrocarbon that remained in the XPS analysis chamber as a contaminant. High resolution transmission electron microscopy (HR-TEM) and selected area electron diffraction (SAED) measurements were carried out by a 200 KV side entry JEOL 2010 TEM.

Results and Discussion

A composition confirmation was carried out by the XPS measurements from as-deposited LiF-MO films. XPS spectra of F 1s peaked at 683.6 eV and Li 1s peaked at 55.6 eV in Figure 1 can be assigned to LiF [18]. XPS signals from transition metals were also detected. Fe 3p, Co 3p and Ni 3p XPS spectra of as-deposited thin films were shown in Figure 2(a), (b) and (c), respectively. The FeO/LiF spectra contain elemental Fe 2p3/2 and 2p1/2 peaks at 706.6 and 720.4 eV, respectively, close to their previously reported values [18,19]. The high-energy shoulder on the metallic Fe peak at 711 eV and the broad satellite peak centered at about 715 eV are characteristic of FeO. Based on the relative intensities of the Fe and FeO peaks, about 30% of the Fe XPS signal arises from metallic Fe, 70% from FeO. For the CoO/LiF thin film, the XPS spectrum includes Co 2p3/2 and Co 2p1/2 binding energies of 778.5 eV and 794.4 eV, respectively, which can be assigned to metal Co. The high-energy

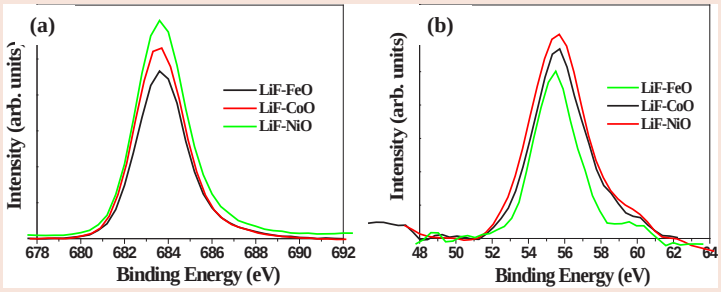

Figure 1: (a) F 1s and (b) Li 1s XPS spectra of the as-deposited nanocomposite LiF-MO thin film.

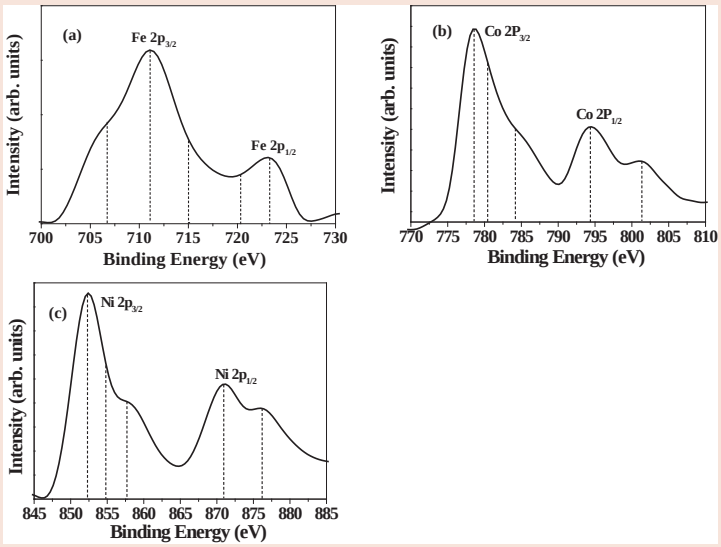

Figure 2: The ex situ (a)Fe, (b) Co, (c) Ni 2p XPS spectra for the as-deposited LiF-MO thin films.

Citation: Liu W, Ke C, Yan X, Duan L, Li L, Liu C (2015) LiF-MO (M=Co, Fe, Ni) Nanocomposite Thin Film as Anode Materials for Lithium-ion Battery. Int J Nanomater Nanotechnol Nanomed 1(1): 014-018. DOI: 10.17352/2455-3492.000004

shoulder on the metallic Co peak at 780.2 eV appears to be associated with a single Co oxide, namely CoO. The satellite peaksat 783.5 and 801.9 eV confirm the presence of CoO [18]. About 35% of the XPS signal was due to metallic Co while 65% was associated with CoO. As was observed in the Fe- based and Co-based films, the metallic Ni 2p3/2 peaks appear close to the expected value of 852.3 eV. The presence of NiO is indicated by the high-energy shoulders on the metallic Ni line at energies of about 854.2 eV and 857.5 eV [18-20]. Metallic Ni accounted for about 40% of the XPS signal with about 60% of the signal arising from NiO. From the above results, the MO/LiF nanocomposites are mainly composed of metallic oxide, LiF and a quantity of metal. The existence of metal is helpful to increase the electric conduction of nanocomposites thin films, and then improve the electrochemical properties of thin film electrodes.

The morphology of the LiF-CoO thin film deposited on a Si substrate was characterized by SEM. The SEM image in Figure 3(a) exhibited a smooth surface and no particles on film surface were observed. As shown in Figure 3(b), the cross-section of the as-deposited LiF-CoO thin film was compact and a uniform thickness of ca. 800nm was observed.

The formation and retention of LiF-MO nanocomposites were supported by ex situ high-resolution TEM images and SAED patterns. Taking the LiF-CoO nanocomposites thin film as example, Figure 4(a) show typical TEM image and SAED patterns shown in the inset for size-controlled LiF-CoO nanostructured electrodes fabricated using the sputtering system, in which the metallic Co and CoO nanoparticles (dark region) are embedded in an amorphous LiF matrix (bright region). The SAED pattern exhibited the clear rings, in which all d-spacing could be assigned to metallic Co and CoO, indicating that the as-deposited thin film mainly consisted of amorphous LiF as well as nanosized polycrystalline metallic Co and CoO. Well-dispersed metallic Co and CoO particles with an average particle size of ca.10 nm were surrounded by the amorphous LiF matrix to form the nanocomposites in the process of sputtering deposition. When thin film electrode was discharged/charged between 0.01 and 3.5V for 10 cycles, the nanocomposites thin film electrodes still preserved the same nanostructure as the as-deposited thin films from the TEM picture shown in Figure 4(b). The nanostructured stability of nanocomposites thin film during the electrochemical cycling indicated that chemical and electrochemical inert LiF matrix can effectively prevent the nanosized CoO particles from agglomerate as we expected.

XRD data were collected to further elucidate the structural properties of the LiF-MO nanostructured electrodes. The presence of polycrystalline Co nanoparticles and amorphous LiF was confirmed by XRD, as shown in Figure 5. Apart from the diffraction peak of $2\theta = 43.60$ corresponding to the stainless-steel substrate, broad peaks of Co (111), Fe (110) and Ni (111) peaked at 44.60, 44.30 and 44.50 was observed in Figure 4, respectively, indicating the existence of

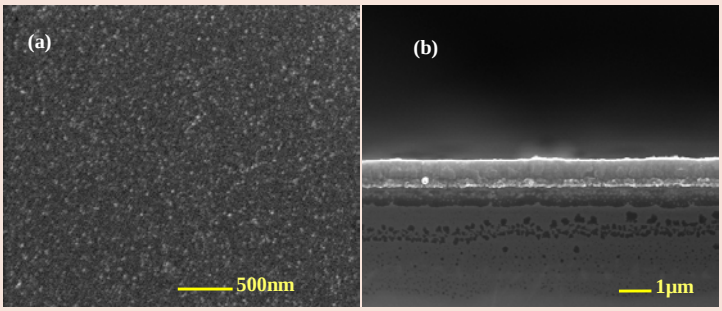

Figure 3: SEM images of the as-deposited LiF-CoO thin film: (a) plane view and (b) corresponding cross-sectional view.

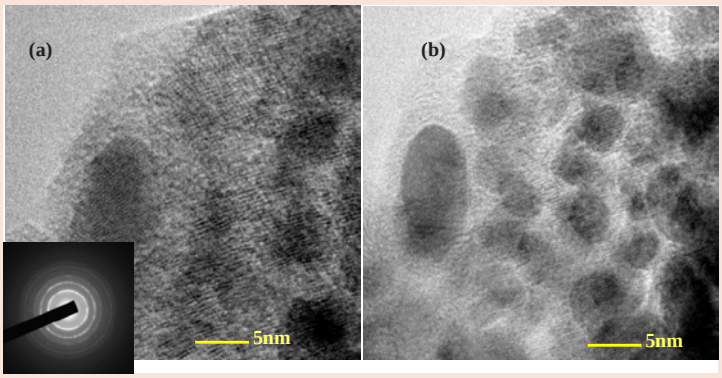

Figure 4: Ex situ high resolution TEM image of (a) the as-deposited LiF-CoO thin film and (b) LiF-CoO thin film after 10 cycles and the corresponding SAED patterns (inset).

Citation: *Liu W, Ke C, Yan X, Duan L, Li L, Liu C (2015) LiF-MO (M=Co, Fe, Ni) Nanocomposite Thin Film as Anode Materials for Lithium-ion Battery. Int J Nanomater Nanotechnol Nanomed 1(1): 014-018. DOI: 10.17352/2455-3492.000004*

metal in the as-deposited thin films [21]. However, the diffraction peaks from metallic oxide were absent, in disagreement with the result of SAED. This may be due to the small particle size of CoO. Moreover, no features of crystalline LiF were observed in the XRD and SAED patterns, confirming the formation of an amorphous phase. Therefore, the structural properties corresponding to both polycrystalline metallic Co and CoO, and amorphous LiF, confirm the existence of two phases within the thin film electrode layer.

Half-cells were assembled by using LiF-MO nanocomposite thin films as positive electrodes and Li metal disk as the negative electrode. These cells were cycled through a Land automatic cycling/data recording system at the current density of 28μA/cm2 between 3.5V and 0.01V. The voltage profiles shown in Figure 6 exhibited different LiF-MO thin film electrode's electrochemical properties. The discharge and charge curves were similar to those of the corresponding transition metal oxides [1-6]. The potential capacity curves of the LiF-MO cells showed some similarities. During the first discharging, the potential rapidly dropped to reach a plateau in the potential region of 0.51.0V, and then continuously decreased down to 0.01V. On the following charging, reversible capacities ranging from 300 to 500mAh/g of LiF-MO were achieved. The well-known mechanisms for these reactions are the reversible reaction of MO+Li →M+Li2O [1]. However, the second discharge curve still kept the same characteristics as the first, which was considerably different from the pure MO electrode reported previously [1-3], indicating that the appearance of LiF matrix in LiF-MO nanocomposites thin film can effectively restrain the structural or textural changes during lithium insertion and extraction. The second discharge capacities of three cells were more than 300 mAh/g, indicating highly active nanocomposites LiF-MO thin films with high specific capacities and good coulombic efficiency. These films were tested for the cycle life test up to 20 cycles as shown in Figure 7. The capacity of the LiF-MO cells on cycling showed the reversible capacity remained constant after the first several cycling. The existence of metal and the stability of nanocomposites in thin film electrode could be responsible for the improvement of thin film's electrochemical properties. The results also show that LiF is suitable for becoming a buffer matrix

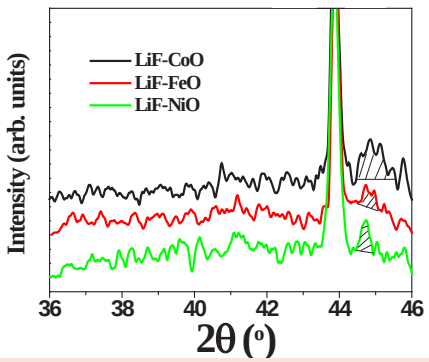

Figure 5: The ex-situ XRD patterns recorded at slow scan speed of 5o/h for the as-deposited LiF-MO thin film (a) M= Fe, (b) M= Co, (c) M= Ni.

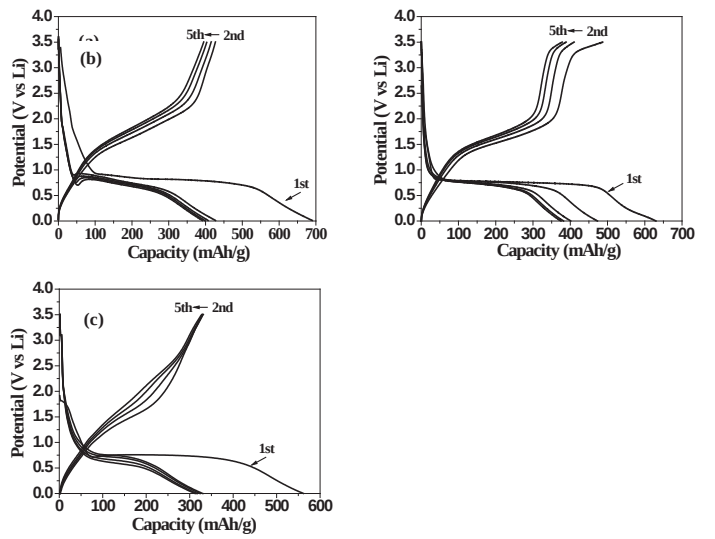

Figure 6: Voltages composition profiles for the as-deposited LiF-MO nanocomposite thin film /LiPF6/Li cells. (a) M= Fe, (b) M= Co, (c) M= Ni.

Citation: *Liu W, Ke C, Yan X, Duan L, Li L, Liu C (2015) LiF-MO (M=Co, Fe, Ni) Nanocomposite Thin Film as Anode Materials for Lithium-ion Battery. Int J Nanomater Nanotechnol Nanomed 1(1): 014-018. DOI: 10.17352/2455-3492.000004*

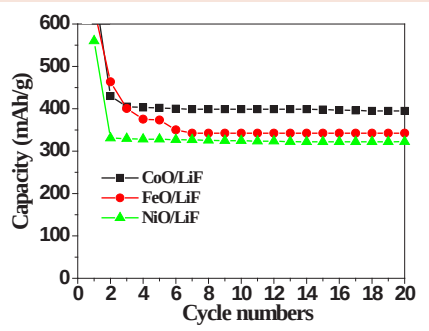

Figure 7: Capacity as a function of cycling number for LiF-MO nanocomposite samples.

to compensate for the expansion and shrinkage of metal oxide during electrochemical cycling, thus preventing the aggregation of nanostructured metal oxide during charging/discharging.

Conclusion

In this review, we provide an overview to provide evidence on the emerging role of HBV pre-S2 deletion mutant protein in HBV tumorigenesis, although cohort studies and genetic studies are needed to clarify whether type II GGHs represent the pre-neoplastic or adenomatous lesions and directly contribute to HCC development. The HBV pre-S2 deletion mutant proteins are retained in the ER and induce ER stress response. Series of ER stress-dependent and -independent growth signals are then activated. Among the diverse pathways, mTOR-mediated signal cascade represent a major mechanism for the disturbed metabolism, genomic instability, and growth advantage, which can potentially drive the type II GGHs toward the pre-neoplastic and neoplastic lesions. To identify the patients at high risk for HCC development represents the major task in combating chronic HBV infection in the coming decades. The development of a DNA chip and ELISA kit for detecting pre-S2 deletion mutant will meet this demand. Chemopreventive or therapeutic agents can then be provided to these high risk HBV carriers to prevent from HCC development.

Acknowledgments

This work was financially supported by the National Nature Science Foundation of China (21103139).

References

1. Poizot P, Laruelle S, Grugeon S, Dupont L, Tarascon JM (2000) Nano-sized transition-metal oxides as negative-electrode materials for lithium-ion batteries. Nature 407: 496-499.
2. Obrovaca MN, Dunlapa RA, Sandersona RJ, Dahn JR (2001) Theelectrochemical displacement reaction of lithium with metal oxides. J Electrochem Soc 48: A576-A588.
3. Poizot P, Laruelle S, Grugeon S, Dupont L, Tarascon JM (2000) From the vanadates to 3d-metal oxides negative electrodes, Ionics 6: p. 321-330.
4. Do J, Weng C (2005) Preparation and characterization of CoO used as anodic material of lithium battery. J Power Sources146: 482-486.
5. Lv P, Zhao H, Zeng Z, Gao C, Liu X, et al.(2015) Self-assembled three-dimensional hierarchical NiOnano/microspheres as high-performance anode material for lithium ion batteries. Appl Surf Sci 329: 301-305.
6. Mukherjee R, Krishnan R, Lu T, Koratkar N (2012) Nanostructured electrodes for high-power lithium ion batteries. Nano Energy 1: 518–533.
7. Huang XH, Tu JP, Zhang CQ (2010) Hollow microspheres of NiO as anode materials for lithium-ion batteries. Electrochim Acta 55: 8981 - 8985.
8. Kim II, Kumta PN, Blomgren GE (2000) Si / TiN Nanocomposites Novel Anode Materials for Li-ion Batteries, Electrochem. Solid-State Lett 3: 493-496.
9. Nazar LF, Goward G, Leroux F, Duncan M, Huang H, et al. (2001) Nanostructured materials for energy storage. Int J Inorg Mater 3: 191–200.
10. Frenning G, Nilsson M, Westlinder J, Niklasson GA, Mattsson M (2001) Dielectric and Li transport properties of electron conducting and non-conducting sputtered amorphous Ta2O5 films. Electrochim Acta 46: 2041–2046.
11. Fu ZW, Li CL, Liu WY, Ma J, Wang Y, et al. (2005) Electrochemical reaction of Lithium with Cobalt fluoride thin film electrode. J Electrochem Soc 152: E50-E55.
12. Zhou YN, Liu WY, Xue MZ, Yu L, Wu CL, et al. (2006) LiF/Co Nanocomposite as a New Li Storage Material. Electrochem Solid-State Lett 9: A147-A150.
13. Liu WY, Fu ZW, Qin QZ (2007) A sequential thin-film deposition equipment for in-situ fabricating all-solid-state thin film lithium batteries. Thin Solid Films 515: 4045-4048.
14. Liu WY, Fu ZW, Qin QZ (2008) A novel “lithium-free” thin film battery with an unexpected cathode layer. J Electrochem Soc155: A8-A10.
15. Huang F, Fu ZW, Chu YQ, Liu WY, Qin QZ (2004) Characterization of Composite 0.5Ag:V2O5 Thin-Film Electrodes for Lithium-Ion Rocking Chair and All-Solid-State Batteries. Electrochem Solid-State Lett 7: A180-A184.
16. Kim II, Blomgren GE, Kumta PN (2003) Nanostructured Si / TiB2 Composite Anodes for Li-Ion Batteries. Electrochem Solid-State Lett 6: A157-A161.
17. 16. Zhang M, Jia MQ, Jin YH, Shi XR (2012) Synthesis and electrochemical performance of CoO/graphenenanocomposite as anode for lithium ion batteries. Appl Surf Sci 263: 573–578.
18. 17. Wagner CD, Riggs WM, Davis LE, Moulder JF, Muilenberg GE (1975) Handbook of X-ray Photoelectron Spectroscopy, Perkin-Elmer Corp.
19. 18. Blanchard P, Grosvenor AP, Cavell RG, Arthur M (2008) X-ray photoelectron and absorption spectroscopy of metal-Rich phosphides M2P and M3P (M=Cr−Ni). Chem Mater 20: 7081–7088.
20. 19. Davidson A, Tempere JF, Che M, Roulet H, Dufour G (1996) Spectroscopic studies of Nickel(II) and Nickel(III) species generated upon thermal treatments of Nickel/Ceria-supported materials. J Phys Chem 100: 4919–4929.
21. 20. Zhong ZY, Liu BH, Sun LF, Ding J, Lin JY, et al. (2002) Dispersing and coating of transition metals Co, Fe and Ni on carbon materials. Chem Physics Lett 362: 135–143.